JOURNAL OF MATERIALS SCIENCE 37 (2002) 3855–3860

Roughness and fractality of nanostructured TiO_2 films prepared via sol-gel technique

P. FALARAS*, A. P. XAGAS
Institute of Physical Chemistry, NCSR "Demokritos", 153 10 Aghia Paraskevi Attikis, Athens, Greece
E-mail: papi@chem.demokritos.gr

Titanium dioxide nanocrystalline thin films were prepared by applying the sol-gel dipping technique using two different titanium (IV) alkoxides: titanium isopropoxide and titanium butoxide. Morphological, structural characterization and examination of the fractal properties were performed by atomic force microscopy (AFM). The effect of the nature of the precursor on the hydrolysis rate and the resulting particle size distribution, roughness, and surface complexity of the TiO_2 films was investigated. Titanium isopropoxide presents higher hydrolysis rates leading to more rough and complex characteristics whereas titanium butoxide films show a relatively smoother surface. Higher fractal dimension values and lower roughness were observed for titania films derived from titanium butoxide. In both cases the obtained films present a complex granular surface network of interconnected particles, suitable for practical applications.

1. Introduction

The growth of metal oxide thin films of controlled surface roughness and complexity presents a significant theoretical and technological importance, offering an exciting opportunity for developing a new class of materials with unique physical, chemical, optical and electronic properties [1]. Titanium dioxide [TiO_2] thin films have recently attracted a particularly increased attention because of their extended use in multitude of applications including photosensitized solar cells [2–8], lithium batteries [9–11], photocatalytic systems [12–14], sensors [15], and electrochromic displays [16, 17].

In all the above applications the usual points raised are related to the shape and order of the nanoparticles that make up the films [18, 19], as well as the surface texture, morphology, spatial extension, roughness, self-similarity, fractality and thickness of the films. These parameters might influence many of the film properties such as chemical adsorption, light absorption and conductivity. Production of open highly porous structures is important because of their high surface area, which allows extensive contact with the reaction medium. At the same time, continuity should exist between nanoparticles in order to prevent traps and dead spots that would deplete the efficiency of the film [18]. The size of the nanoparticles is an additional important parameter that affects the electronic properties and the absorption onset of the nanocrystallites and should be carefully taken into account [20].

It then obvious that the performance and efficiency of the devices based on titanium dioxide thin films will strongly depend on the semiconductor surface properties and especially on the preparation conditions. Among the existing thin film fabrication methods, the sol-gel coating technique has been receiving renewed interest, largely attributed to the fact that it combines a number of specific advantages, such as the potential for large area coverage, simplicity, reproducibility, low cost and good mechanical properties [21, 22].

Titnium dioxide thin films can be prepared by the sol-gel technique, where metal alkoxides $Ti(OR)_4$ (R = alkyl groups) are generally used as principal precursors. Further hydrolysis creates clusters containing many oxide molecules and subsequent polymerization causes the formation of a three-dimensional network with octahedral TiO_6 coordination. There have been several reports about the formation of sol-gel TiO_2 thin films and it is now well established that the choice of the precursor strongly influences the final film properties. A variety of Ti-containing organic precursor materials have been used, and Ti-isopropoxide and Ti-butoxide are among the most promising of them. Thus, it has been confirmed that the chemical reactivity of the ligand groups initially coordinated on the titanium precursor plays a decisive role in the structure development of as-deposited sol-gel TiO_2 films [23]. However, no special attention was paid to the comparison, improvement and optimization of the obtained films in terms of roughness, nanostructure and surface complexity, parameters which control the optical and electronic properties and account for the performance of the material in a number of potential applications. In this contribution, from a comparative point of view, we emphasize on

*Author to whom all correspondence should be addressed.

the preparation and characterization of rough, fractal, large surface area nanocrystalline titanium dioxide thin films with highly controllable parameters derived from Ti-isopropoxide and Ti-butoxide precursors trying to determine, especially by AFM, at which extent the nature of the ligand group in titanium precursors affects their surface properties.

2. Experimental

The significance of the hydrolysis rate was pointed out by using two different titanium alkoxide precursors $Ti(OR)_4$: titanium isopropoxide [$Ti(O\text{-}i\text{-}C_3H_7)_4$] (TIP) and titanium butoxide [$Ti(O\text{-}n\text{-}C_4H_9)_4$] (TB) (Aldrich), which differ only in the –R group and keeping all other parameters effecting the film's properties constant (e.g., viscosity, pH, concentration, temperature, solvent). For the preparation of the dipping solution titanium alkoxide (1.1 g and 1.3 g respectively) was added dropwise (in order to avoid the formation of large agglomerates, due to local excess of the precursor) in 10 ml of a 7 : 10 ethanol/isopropanol mixture, under vigorous stiring [24, 25]. To this solution a drop of 3N HCl was added as the catalyst. Upon acid addition, a homogeneous semi-transparent sol was formed and subsequently, the reaction mixture was left standing to peptize for 12 h prior to deposition, finally forming a clear solution. The solution was coated uniformly over the glass substrate surface by dipping the substrate into the solution and lifting it at a controlled speed. During the whole process, the room temperature was kept constant at 20°C. The films were then deposited by dip-coating process on microscope glass substrates and subjected to heat treatment (drying at 100°C for 15 min and the sintering at 500°C for 30 min in order to remove organic components).

Thickness measurements were performed using a Sloan Dektak II Stylus profilometer. The film crystallinity was analyzed with an X-ray diffractometer (Siemens D-500, Cu-K_a radiation) after annealing at 150°, 300° and 550°C and by Raman spectroscopy (DILOR OMARS 89 spectrometer). Surface morphology, roughness and fractality of the films were examined with a Digital Instruments Nanoscope III atomic force microscope (AFM), operating in the tapping mode (TM). For the fractal analysis the V423r3 algorithm was used.

3. Results and discussion

Depending on the withdrawal speed different thickness can be attained: a speed of 1 cm/s gives rise to a mean thickness of 0.8 μm per dip while a speed 0.5 cm/s yields an average thickness 0.4 μm/dip, Fig. 1. So, in order to achieve a film thickness of several μm, a 5 times repetition of the cycle was essential. By this method, TiO_2 films exhibiting very good adherence on the glass substrates were obtained. Optical microscopy did not show pinholes and micro cracks. However, Scanning Electron Microscopy (SEM) analysis ($\times$1000, $\times$ 5000, $\times$ 10000 and $\times$ 20000 magnification images) confirmed the presence of a microporous open structure of interconnected particles [26].

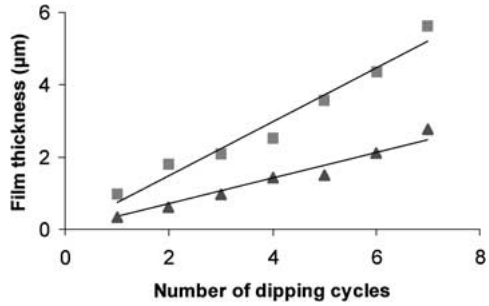

Figure 1 The relationship between the coating thickness and the number of coating cycles under a withdrawal speed of 1 cm/s (squares) and 0.5 cm/s (triangles). Sintering temperature 500°C.

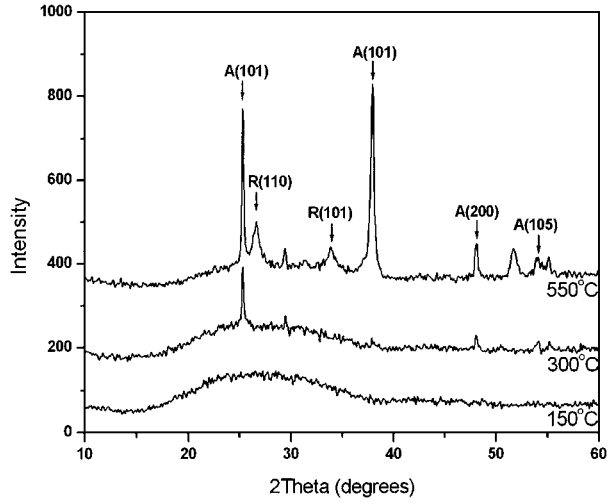

Figure 2 X-ray diffraction patterns of a TIP film annealed at different temperatures: from bottom to above: 150°, 300°, and 550°C; A = anatase, R = rutile.

By X-ray diffraction it has been confirmed that both TIP and TB films exhibit similar behavior upon thermal treatment. Fig. 2 shows the X-ray diffraction patterns of the as-deposited and annealed TIP TiO_2 films. It can be seen that at low temperatures the films are amorphous. With increasing temperature the amorphous phase is crystallized into anatase [27]. In fact, under these specific preparation conditions, the films are comprised of single anatase and no trace of the rutile phase was detected in the XRD pattern for temperatures below 450°C. Raman spectroscopy confirmed the existence of anatase main vibration peaks at 148 cm^{-1} (E_g, very strong), 397 cm^{-1} (B_{1g}, strong), 516 cm^{-1} (B_{1g}/A_{1g}, strong) and 638 cm^{-1} (E_g, strong) respectively [26]. This observation, is of great importance since it has been repeatedly established that anatase is more favorable for energy conversion applications [28]. On the contrary, thermal treatment to 550°C leads to films presenting both the anatase and rutile diffraction peaks, Fig. 2.

The fundamental chemical process involved in sol-gel is based on hydrolytic and condensation reactions, which lead to the formation of macromolecular networks. If hydrolysis proceeds slowly (e.g., in dilute solutions) or the dipping is performed in a "premature" stage, the resultant films are very thin, relatively smooth, non-light absorbing and improper for solar cell applications. On the other hand, very high

hydrolysis rates are also unfavorable since they lead to the formation of large aggregates and consequently to quick precipitation. If the dipping is performed at a later stage, when polymerization has proceeded and the sol has reached a high viscosity state, relatively thick films are produced (>1–$2\ \mu$m) which tend to crack and peel off readily. Moreover, by this means, the sol reaches the gelation stage very fast, which is unfavorable for industrial coating applications (low "shelf life"). These observations clearly imply that the films properties and surface roughness derive from a balance of some factors playing a competing role.

Since the mechanism of the polymerization follows S_{N^2} type, including a nucleophilic attack of the titanium metal center, steric hindrance by the presence of the alkyl groups is expected to play a crucial role. Thus, the more bulkier butoxide ligand is expected to impede the access to the titanium atom, inhibiting by this means the propagation of the hydrolysis, more than the less bulky isopropoxide. Another additional factor contributing to the slower rate for the butoxide precursor is the formation of oligomeric structures (usually dimers and trimers) [29, 30].

Atomic force microscopy, a mechanical technique following "in relief" the surface morphology has been demonstrated to be a very versatile and powerful tool for surface imaging at the submicrometer level and the revelation of surface characteristics of Titanium dioxide thin films [24]. In Figs 3 and 4 top view and three-dimensional surface plots (600×600 nm) AFM representations are presented for the TIP and TB films respectively. The TIP films are composed of relatively large interconnected particles (the minimum grain diameter 'φ' is about 25 nm) and pores, building up high

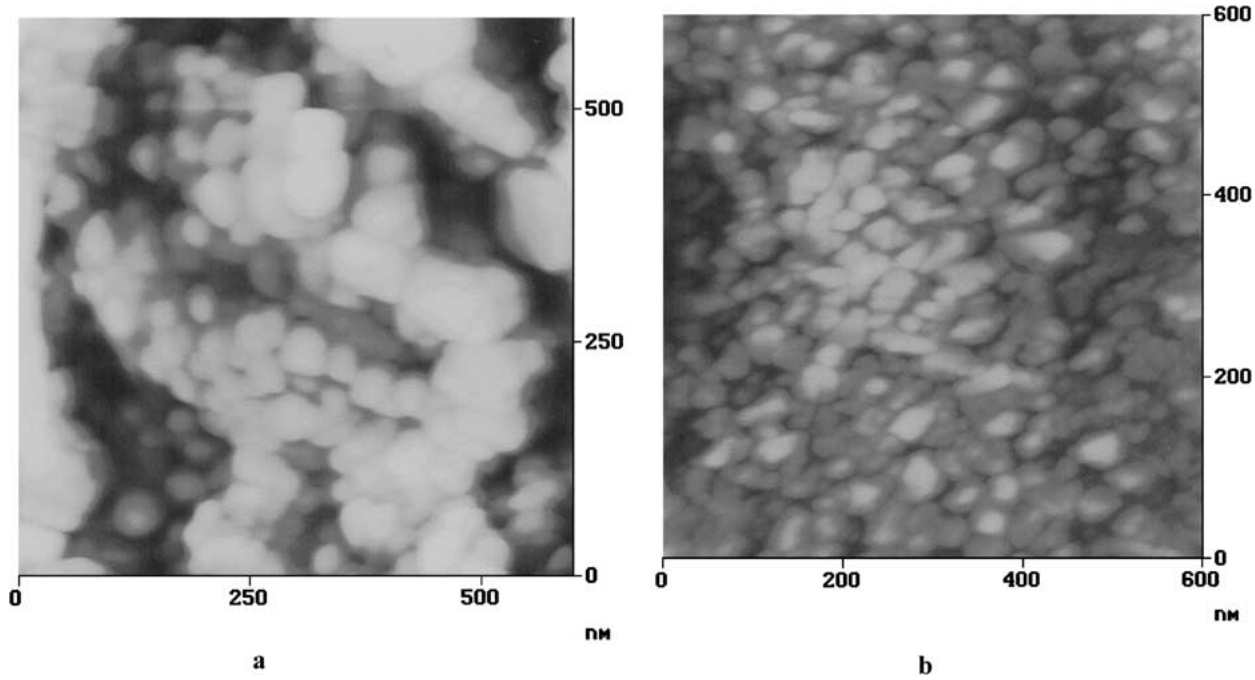

Figure 3 Top view AFM images (tapping mode) of sol-gel deposited TIP (a) and TB (b) TiO_2 films (scan range 600×600 nm) sintered at 500°C.

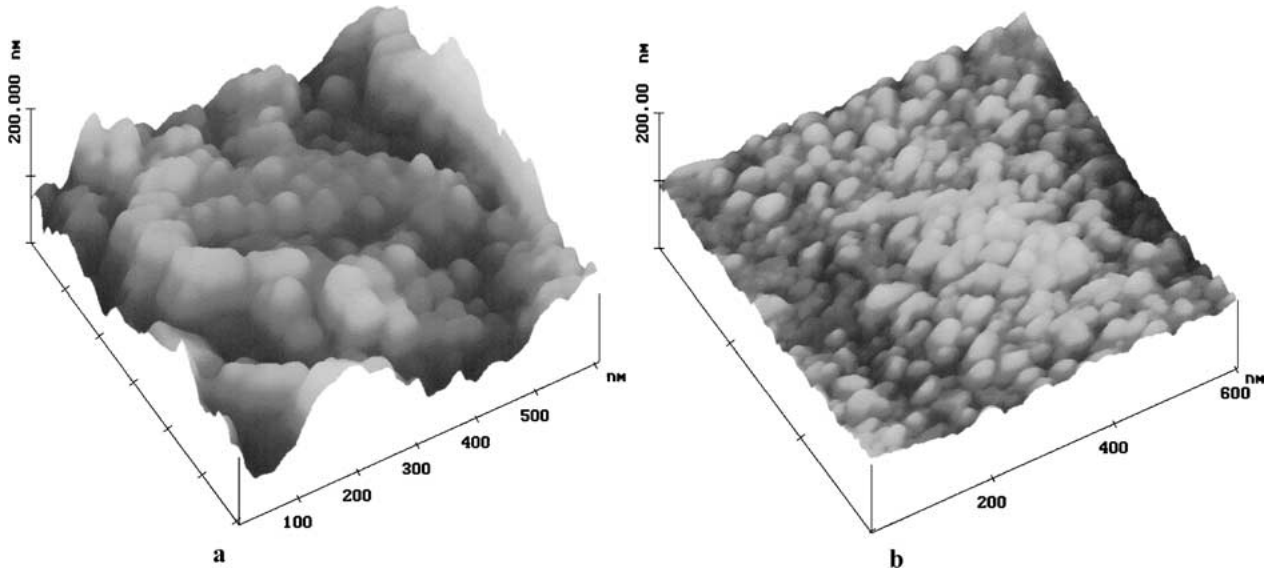

Figure 4 3D AFM images (tapping mode) of sol-gel deposited TIP (a) and TB (b) TiO_2 films (scan range 600×600 nm) sintered at 500°C.

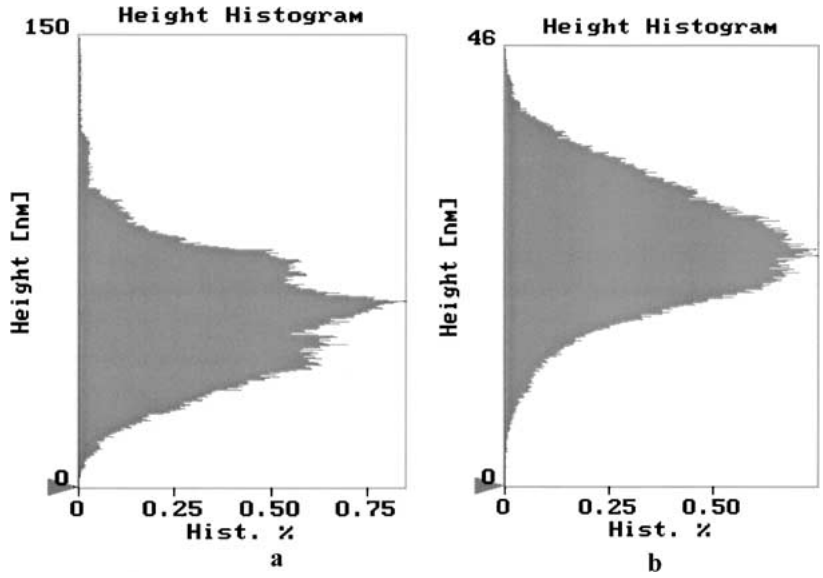

Figure 5 Grain size distribution (height histogram) for TIP (a) TB (b) sol-gelnTiO$_2$ films sintered at 500°C.

"mountains" and deep "valleys". The TB films on the contrary exhibit a finer microstructure and consisted of smaller and more uniform grains ($\varphi = 13$ nm) forming a rather flat but more complex surface texture which is consistent with a much less rough topography. It is important to note that the grain diameter values obtained by AFM are comparable to the ones calculated from the XRD spectra by applying the semi-empirical Scherrer equation on the 25.4° peak (101). The above analysis has given particle sizes of 35 nm and 15 nm for TIP and TB films respectively.

Grain size analysis has shown that height distributions of surface characteristics for both films are Gaussian-like, Fig. 5. Generally, the TIP films present surface characteristics of greater height. The height distribution histogram of the TIP films is obviously broader (sizes ranging from 20 to 90 nm) from the corresponding TB curve (range 10–50 nm). The height distribution maximum of the TB film is quite well defined (35 nm) while TIP displays more a broad maximum (at about 40–60 nm). Such a difference can be reflected in the rms roughness values (rms = root mean square = the standard deviation of the Z values, Z being the total height range analyzed) of the two films, which were measured 19.7 nm (TIP films) and 6.4 nm (TB films) respectively, Table I. Therefore it can be concluded that the broader the size distribution is, the rougher are the resulting films. This important observation can be explained by considering that in the case of mono-dispersed particles, a better packing of the particles is favored, leading to the formation of a less porous structure and morphology (TB films).

TABLE I Minimum grain diameter, roughness and fractal dimension of TIP and TB Sol-Gel TiO_2 thin films sintered at 500°C

TiO_2 films	Mean grain diameter φ (nm)	Roughness rms (nm)	Fractal dimension, D_f
TIP	25	19.7	2.12
TB	13	6.4	2.31

Besides the surface roughness, the film fractal dimensions can be also measured using AFM microscopy. Thus, in order to evaluate and compare the geometric complexity of the film surfaces, qualitative analysis including measurements of parameters such as feature frequency and fractal dimension D_f ($3 \geq D_f \geq 2$) was performed. An analytical presentation of fractal analysis in TiO_2 films is given in [31]. For calculating the fractal dimension (a parameter which reflects the scaling behavior and is an intrinsic property of the material) of a surface, several techniques may be applied. The one used in this work divides the three-dimensional film surface into a series of triangles. The size **L** of triangles is varied and the surface area of each triangle is calculated and recorded for each size **L**. The logarithmic plot of the cell size versus the surface area determines the fractal value of the surface (the fractal dimension D_f is defined as the slope of the line obtained by plotting the log of the cell size versus the log of the cell surface area).

The fractal analysis performed, Fig. 6, has shown that the as-prepared films exhibit also self-affine character over a significant range of length scales as a consequence of a "chaotic" dynamic deposition process, very sensitive to the initial alkoxide precursor. It is worthwhile mentioning that the TB films have higher fractal dimension D_f than the TIP films, Table I. The measured values were 2.31 (±0.02) and 2.12 (±0.02) respectively. This difference can be explained taking into account the fact that the fractal dimension D_f characterizes mainly the complexity of the surface and not its roughness. The TB TiO_2 films present a more complex topography characterized by a greater number of surface features of higher frequency and consequently, their effective surface extension is expected to be several hundred times greater than their geometric one [31].

Such high surface area fractal TiO_2 films may have important applications in photochemical and solar energy conversion processes. Recently, the fractal characteristics of TiO_2 nanocrystalline films were studied

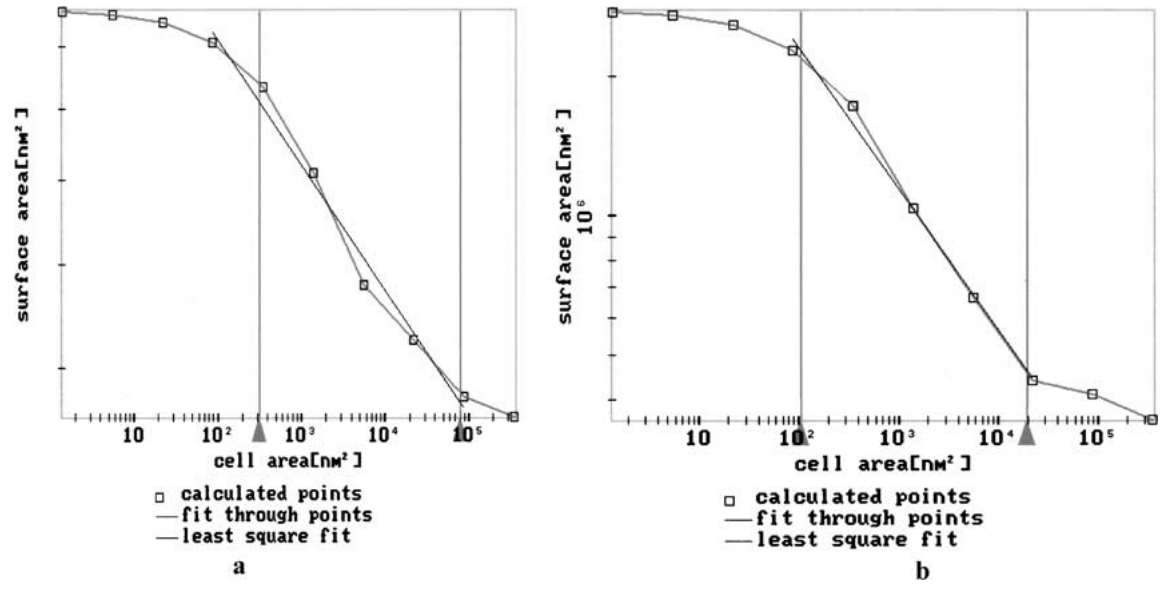

Figure 6 Fractal analysis on TIP (a) and TB (b) sol-gel TiO_2 films sintered at 500°C.

and related to the efficiency of light absorption [8, 32]. It has been proved that the light-receiving surface may be hundreds of times larger than the geometric area and efficient energy captivation takes place, which considerably increases the rate of photochemically, and photoelectrochemically induced reactions.

4. Conclusions

An investigation of the conditions under which uniform nanocrystalline thin TiO_2 films are formed via the sol-gel dipping method using titanium isopropoxide and titanium butoxide precursors has led to the following conclusions:

- The surface properties (parameters, such as size of nanoparticles, surface roughness, morphology, fractal dimension, and spatial extension) of the films strongly depend on the choice of the alkoxide. Higher hydrolysis rates obtained by using titanium isopropoxide lead to poly-dispersed particle sizes. The roughness of the deposited films can be tailored by controlling the hydrolysis rate. A narrow size distribution of the film particles leads to relatively smooth films while a large poly-dispersed one leads to more rough and textured films.
- The film's surface complexity derives from a competitive balance of a number of factors, one of them being the alkoxide precursor. The use of titanium butoxide leads to films with higher values of fractal dimension. This is very important for applications where large surface area films are required. In fact, novel applications and/or more efficient devices based on light absorption or chemical adsorption, which will take into advantage the self-similar character of fractal surfaces, will be developed.

Acknowledgements

Financial support from NCSR Demokritos and from the Greek General Research Secretariat GSRT is greatly acknowledged. The authors are indebted to F. Papadimitriou for her invaluable assistance in obtaining the AFM images and to I. M. Arabatzis for his precious help during the revision of this manuscript.

References

1. P. MEAKIN, *Phys. Rep.* **235** (1993) 191.
2. S. M. ZAKEERUDDIN, M. K. NAZZEERUDDIN, P. PÉCHY, F. P. ROTZINGER, R. HUMPHRY-BAKER, K. KALYANASUNDARAM, M. GRÄTZEL, V. SHKLOVER and T. HAIBACH, *Inorg. Chem.* **36** (1997) 5937.
3. B.'O. REGAN and M. GRÄTZEL, *Nature* **353** (1991) 737.
4. A. ZABAN, O. I. MICIC, B. A. GREGG and A. J. NOZIK, *Langmuir* **14** (1998) 3153.
5. R. W. FESSENDER and P. V. KAMAT, *J. Phys. Chem.* **99** (1995) 12902.
6. R. ARGAZZI, C. A. BIGNOZZI, T. A. HEIMER, F. N. CASTELLANO and G. J. MEYER, *J. Phys. Chem.* **101** (1997) 2591.
7. F. CAO, G. OSKAM and P. C. SEARSON, *ibid.* **99** (1995) 17071.
8. P. FALARAS, A. P. XAGAS and A. HUGOT-LE-GOFF, *New J. Chem.* (1998) 557.
9. S. Y. HUANG, L. KAVAN, I. EXNAR and M. GRÄTZEL, *J. Electrochem. Soc.* **142** (1995) L38.
10. L. KAVAN, M. GRATZEL, J. RUTHOUSKY and A. ZUKAL, *ibid.* **143** (1996) 2.
11. P. KRTIL, L. KAVAN and D. FATTAKHOVA, *J. Solid State Electrochem.* **1** (1997) 83.
12. J. YU, X. ZHAO, J. DU and W. CHEN, *J. Sol-Gel Science & Techn.* **17** (2000) 163.
13. A. FUJISHIMA, K. HASHIMOTO and T. WATANABE, "TiO_2 Photocatalysis, Fundamentals and Applications" (Bkc Inc, Tokyo, 1999).
14. A. FUJISHIMA, T. N. RAO and D. A. TRYK, *J. Photochem. Photobiol. C: Photochem. Rev.* **1** (2000) 1.
15. S. COSNIER, A. SENILLOU, M. GRÄTZEL, P. COMTE, N. VLACHOPOULOS, N. J. RENAULT and C. MARTELET, *J. Electronal. Chem.* **469** (1999) 176.
16. Y. YONGHONG, Z. JIAYU, G. PEIFU, L. XU and T. JINFA, *Thin Solid Films* **298** (1997) 197.
17. N. OZER and C. M. LAMPERT, *Sol. Energy Mater. Sol. Cells* **54** (1998) 147.
18. R. A. CARUSO, M. GIERSIG, F. WILLIG and M. ANTONIETTI, *Langmuir* **14** (1998) 6333.

19. S. D. BURNSIDE, V. SHKLOVER, C. BARBE, P. COMTE, F. ARENDSE, K. BROOKS and M. GRATZEL, *Chem. Mat.* **10** (1998) 2419.
20. L. BRUS, *J. Phys. Chem.* **90** (1986) 2555.
21. A. CHEMSEDDINE and T. MORITZ, *Eur. J. Inorg. Chem.* (1999) 235.
22. O. LEGRINI, E. OLIVEROS and A. M. BRAUN, *Chem. Rev.* **93** (1993) 671.
23. C.-C. TING and S.-Y. CHEN, *J. Mater. Res.* **16** (2001) 1711.
24. A. P. XAGAS, E. ANDROULAKI, A. HISKIA and P. FALARAS, *Thin Solid Films* **357** (1999) 173.
25. A. P. XAGAS, M. C. BERNARD, A. HUGOT-LE GOFF, N. SPYRELLIS, Z. LOIZOS and P. FALARAS, *J. Photochem. Photobiol. A: Chem.* **132** (2000) 115.
26. A. P. XAGAS, PhD Thesis, Athnes, Greece (2001).
27. JCPDS Powder Diffraction File, JCPDS (Information Centre for Diffraction Data, Sworthmore, PA, 1980), Card 21-1272.
28. S. J. TSAI and S. CHENG, *Cat. Today* **33** (1997) 227.
29. A. N. OZERIN, E. YU. SHAPIROV, L. A. OZERINA, N. V. GOLUBKO and M. I. YANOVSKAYA, *Rus. J. Phys. Chem.* **73** (1999) 277.
30. F. BABONNEAU, S. DOEUFF, A. LEAUSTIC, C. SANCHEZ, C. CARTIER and M. VERDAGUER, *Inorg. Chem.* **27** (1988) 3166.
31. A. PROVATA, P. FALARAS and A. P. XAGAS, *Chem. Phys. Lett.* **297** (1998) 484.
32. P. FALARAS, *Solar Energy Materials and Solar Cells* **53** (1998) 163.

Received 19 November 2001
and accepted 14 May 2002